International Journal of Research and Review
[Indexed, Peer-Reviewed Journal]
Volume 13; Issue: 1; January 2026
Website: www.ijrrjournal.com
Research Paper *E-ISSN: 2349-9788; P-ISSN: 2454-2237*

Study of the Thermomechanical Behavior of a Mixture of Two Aluminosilicate Powders

Banzouzi Samba Vivien Igor[1,2], Nzaba-Madila Erman-Eloge[3], Vezolo Stanislas Prudence[2], Bibila Mayaya Bisseyou Yvon[4], Moutou Jospeh-Marie Saint Bastia[2], Elimbi Antoine[5]

[1]Faculty of Applied Sciences, Denis SASSOU N'GUESSO University, Kintélé, Republic of Congo
[2]Laboratory of Inorganic and Applied Chemistry, Faculty of Science and Technology, Marien N'GOUABI University, Brazzaville, Republic of Congo
[3]University of Quebec at Trois-Rivières, Trois-Rivières, Quebec, Canada
[4]Laboratory of Applied Inorganic Chemistry, Faculty of Science, University of Yaoundé I, Yaoundé, Cameroon
[5]Laboratory of Materials, Environment, and Solar Energy Sciences, UFR SSMT, Félix Houphouët-Boigny University, Abidjan, Côte d'Ivoire

Corresponding Author: Banzouzi Samba Vivien Igor

DOI : https://doi.org/10.52403/ijrr.20260135

ABSTRACT

This work focused on studying the thermomechanical behavior of a mixture of two aluminosilicate powders. The particle-size distribution of the mixture was determined by wet sieving. The mixture of aluminosilicate powders was characterized by its plasticity (Atterberg limits), as well as its chemical and mineralogical composition (XRD) and microstructure (SEM). Shrinkage before and after firing was measured. Water absorption rates and three-point flexural strength were also determined. Mixtures M1, M2, M3, M4, and M5 were formulated and showed moderate shrinkage, with plasticity indices (24, 27, 31, and 33%) below 35%, making them suitable for extrusion. The addition of sodium hexametaphosphate to the slips prepared from the mixtures decreased the pH (from 5.85 to 4.23) and promoted particle flocculation. The addition of sodium metasilicate increased the pH from 4 to 8.7, enhanced dispersion, and resulted in a stable slip. The diffractograms of the ceramic products were obtained at firing temperatures of 1100 and 1150°C. Mullite was clearly present after the thermal treatment of the mixtures, and the degree of crystallinity was significant. At 1150°C, mixture ND2 exhibited a flexural strength of 11.97 MPa, a water absorption rate of 6.82%, and a shrinkage of 4.53%, compared to ND1 at the same temperature, which showed a flexural strength of 9 MPa, a water absorption rate of 10.03%, and a shrinkage of 2.85%.

Keywords: Clay mixture; determination; technological and mechanical properties; Ntokou; Dongou.

1. INTRODUCTION

Aluminosilicate ceramics are composed of clays, with kaolinite remaining the most widely used mineral species throughout time. It is highly sought after in large-scale ceramic production (such as construction materials), which occupies a prominent place in the global ceramics market (Lecomte et al., 2004). Their abundance and especially their low production cost justify their widespread use.

However, many ceramics produced from clay-based materials are often composed of natural mixtures of minerals whose particle-size distribution and physicochemical properties vary considerably. The nature of the final ceramic product depends on several

parameters, including the characteristics of the raw materials used and the behavior of the clay during the various stages of the ceramic manufacturing process.

In the Republic of Congo, clay-based earthenware is mainly used for the production of traditional construction materials (earthen bricks), pottery items (water jars, dishes, etc.), and handicrafts. This industry remains largely artisanal. As a result, many Congolese consumers rely on imported porcelain, sanitary ware, plates, tiles, and wall and floor coverings (El Boukili et al., 2021). This situation is largely due to the lack of in-depth studies on the raw materials used.

The present work aims to promote the valorization of local clay materials.

Indeed, as part of its policy to diversify the Congolese economy, the government has initiated the establishment of several cement production units in Bouansa (Bouenza Department) and Loutété (Pool Department), as well as ceramic complexes in Maloukou (Pool Department) and Makoua (Cuvette Centrale Department).

To support this initiative, we conducted a research mission in the locality of Ntokou, located near Makoua in the Cuvette Centrale Department. The abundance, availability, and low transportation cost (Ntokou–Makoua) of clay raw materials justify the choice of Ntokou as the study area.

The general objective of this work is to study the thermomechanical behavior of a mixture of two aluminosilicate powders. The particle-size distribution of the mixture will be determined by wet sieving and sedimentation. The maximum water content and plasticity will be assessed using the Atterberg limits. Structural analysis and microstructure will be investigated using XRD and SEM. The technological potential and properties of the mixture will also be evaluated.

2. MATERIALS AND METHODS

This section presents the geographical location of Dongou and the methodology required to conduct the present study.

2.1. Geographical locations of Ntokou and Dongou

- Ntokou is a district of the Cuvette Department, with geographical coordinates 0°01’35’’N and 16°20’02’’E. It is located on the right bank of the Likouala-Mossaka River, approximately 14 hours by canoe from Makoua. By road, it is less than 40 km from Makoua. The sampling site, Yombe, is located less than 1 km from the Likouala-Mossaka River, specifically in a forest known as Andziga. The clay material (NTO) used in this study was collected at a depth of 1.5 m (altitude: 324 m; coordinates: 00°01’09.2’’N, 015°55’42.1’’E).
- Dongou clay soil was collected in the Likouala Department, specifically in the Mbala district of Dongou. The sample was taken at a depth of 50 cm and a height of about 4 m. The area had not undergone any prior treatment.

2.2. Characterization methods

The Atterberg limits were measured according to standards NF P 94-051 (Afnor, 1993). The proportions of particle-size classes were determined according to standards NF P 94-056 (Afnor, 1996). X-ray diffractograms were recorded at the Ceramic Technology Transfer Centre (CTTC) in Limoges using a PANalytical X’Pert PRO diffractometer with a copper Kα radiation source (Brindley et al., 1980). Major-element chemical composition was determined at the Dangote laboratory in the Republic of Congo. The heating rate was set at 5°C/min, with a maximum temperature of 1150°C. Cooling occurred freely according to the thermal inertia of the furnace.

2.3. Technological properties

2.3.1. Linear shrinkage

Shrinkage refers to the reduction in the dimensions of a material compared to its initial values after drying or thermal treatment. When shrinkage concerns variation along a single dimension, as in this study, it is referred to as linear shrinkage (LS). In this work, linear shrinkage was

measured along the length of parallelepiped specimens. Measurements were taken using a caliper (ROCH France, patented S.G.D.G.).

Linear shrinkage is given by the following relation:

$$SL(\%) = \frac{Lo-Lf}{Lo} \times 100 \; ; \quad SW(\%) = \frac{Wo-Wf}{Wo} \times 100 \quad ; \quad ST(\%) = \frac{To-Tf}{To} \times 100. \qquad (1)$$

Voici la traduction claire et scientifique de ton passage :
Where:
SL: Shrinkage in length;
SW: Shrinkage in width;
ST: Shrinkage in thickness.
L_o, W_o, and T_o are the length, width, and thickness before thermal treatment, respectively.
Lf, Wf, and Wf are the length, width, and thickness after firing, respectively.

2.3.2. Water Absorption Percentage

The water absorption coefficient (Wac), or the percentage of absorbed water, is defined as the ratio between the increase in mass caused by partial water saturation and the dry mass (Dm) of the material. This measurement is carried out on cylindrical specimens. Partial saturation is obtained by fully immersing the sample in demineralized water while the system is brought to and maintained at boiling for two hours under atmospheric pressure. After 24 hours of cooling at ambient temperature, the sample is removed from the bath, gently blotted with fine absorbent paper, and weighed to determine its wet mass (Wm).
The water absorption percentage is given by the following relation:

$$Wac = \frac{Wm-Dm}{Dm} \times 100 \qquad (2)$$

Where:
Wm = wet mass
Dm = dry mass

2.3.3. Three-Point Flexural Strength

This test is used to measure the breaking strength of a material. The EZ20 testing device is used, with a crosshead displacement speed of 0.35 mm/s. A prismatic specimen of the material is placed on two supports, and an increasing force is applied at the center of the specimen until rupture. The distance between the supports is 80 mm (Figure 1) (NF EN 843-1; Duplan et al., 2021).

$$\sigma(MPa) = \frac{3\,F(N)\times L(mm)}{2\,b(mm)\times h2(mm)} \qquad (3)$$

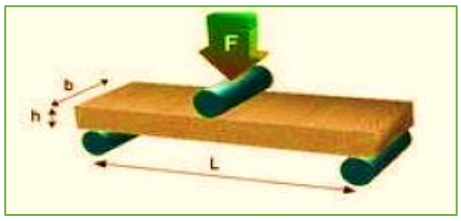

Figure 1: A specimen under three-point bending.

3. RESULTS

This section presents the results related to the addition of Dongou clay to Ntokou clay, as well as the thermal behavior of the Ntokou–Dongou clay mixtures (Mi, with i = 1 to 5).
The high sand content in Ntokou clay significantly affects its plasticity, making it unsuitable for use in modern ceramic industries, as demonstrated by the Winkler diagram. In contrast, Dongou clay contains barely 2% sand and is therefore considered highly plastic. Due to this property, it was selected to improve the physical characteristics of Ntokou clay by adding it in precise mass proportions (5%, 10%, 15%, 20%, and 25%). Both Ntokou and Dongou clays have already been characterized (Moutou et al., 2020; Bibila et al., 2025).

3.1. Geotechnical Analysis

3.1.1. Particle-size distribution and Atterberg limits

Table 1 shows the particle-size distribution and Atterberg limits of Ntokou clay (NTO),

Dongou clay (DON), and their mixtures (M1, M2, M3, M4, and M5).

Table 1: Particle-size distribution and Atterberg limits of the different samples

Sample	<2µm (%)	2-20 µm (%)	>20µm (%)	Liquid limit (%)	Plasticity limit (%)	Plasticity indice (%)
NTO	28	20	52	40	16.9	23.2
DON	62	36	2	70.1	30.1	40
M1	52.5	20.8	26.7	43	19	24
M2	53	21.6	25.4	47	20	27
M3	53.5	22.4	24.1	53	21	31
M4	54	23.2	22.8	55	22	33
M5	54.5	24	21.5	67	30	37

Thanks to this particle-size distribution, the different samples were plotted on the Winkler Diagram. Figure 2 shows the positioning of the various samples on the Winkler Diagram.

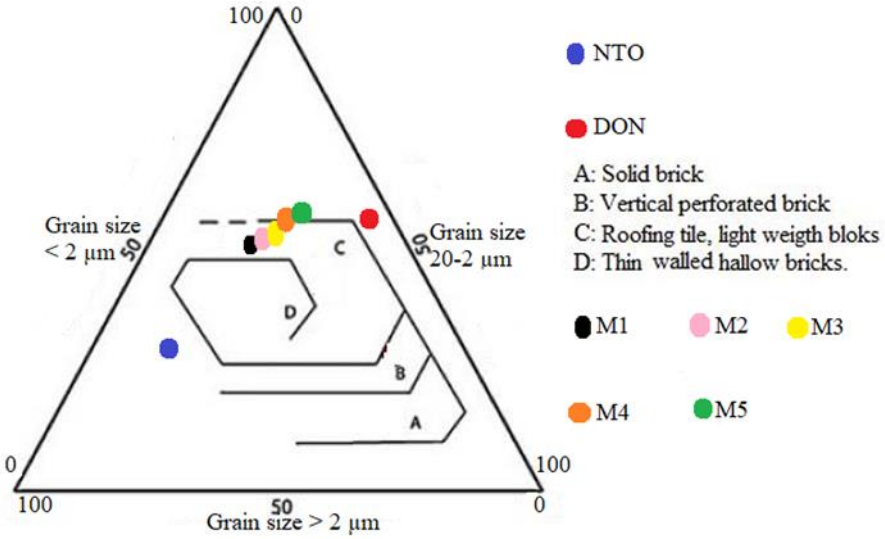

Figure 2: Positions of NTO, DON, and the mixtures on the Winkler Diagram (Capitâneo et al., 2005).

M1 and M2 are located in the same zone as NTO; M3 and M4 are very close to the boundary between the light block tile zone and the "no use" zone. M5 falls within the "no use" zone, like DON.

The positioning of M5 indicates that it cannot be used for the production of earthenware products. The M5 mixture contains only 25% DON clay. However, DON clay, with 62% of particles smaller than 2 µm, has a strong influence on NTO clay. This is confirmed by the values shown in Table 1: from mixture M3 to M5, as the clay content increases, the sand content decreases. Consequently, mixtures M3, M4, and M5 can be used for the manufacture of ceramic products (tiles, roof tiles, porcelain, etc.) (Samara et al., 2007).

Table 1 also presents the Atterberg limits of NTO and DON clays, as well as those of the resulting mixtures. These data allowed us to position the different samples on the Casagrande Diagram (Figure 3). These results are also interpreted using the Casagrande Diagram, which provides information on the plasticity of the clays.

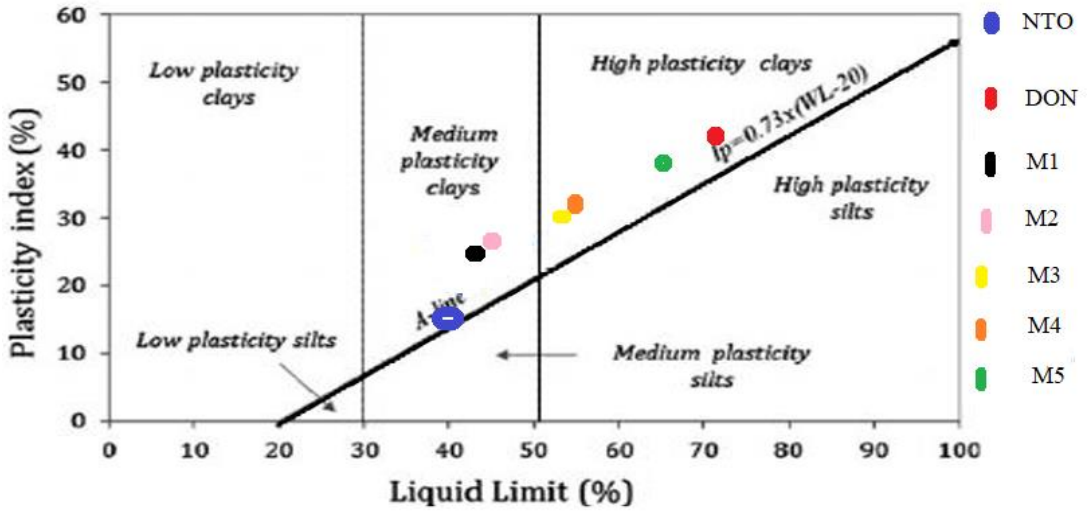

Figure 3: Positioning of NTO, DON, and the mixtures on the Casagrande Diagram (Casagrande et al., 1948).

We observe that the samples NTO, M1, and M2 belong to the category of medium-plasticity clays, due to their liquid limits being below 50%. On the other hand, the samples DON, M3, M4, and M5 are classified as highly plastic clays, as they have a high plasticity index (over 35%) and liquid limits above 50%. This high plasticity of M3, M4, and M5 is explained by the clay content (62%) found in DON during the particle-size analysis.

Thus, the addition of DON to NTO positively influences the plasticity of NTO, with the plasticity index increasing from 23% to 37%. This is confirmed by the position of M5 on the Casagrande chart.

Based on the different plasticity indices of the samples M1, M2, M3, M4, and M5, and their positions on the workability map (Figure 4), we can estimate the molding properties of these clay soils.

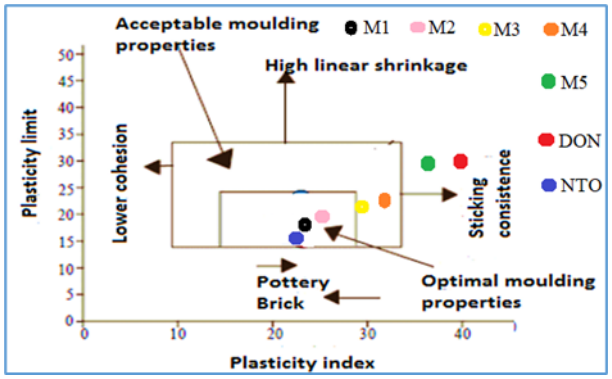

Figure 4: Positions of the samples NTO, DON, M1, M2, M3, M4, and M5 on the Workability Map (Bain et al., 1978).

Samples M1 and M2 exhibit optimal molding properties; M3 and M4 have acceptable molding properties. Sample M5 falls within the high-plasticity zone. This positioning indicates that the plasticity increase of NTO clay was successful.

However, sample M5 is not suitable for extrusion, as its plasticity index exceeds 35%. Extrusion is a process used in the production of tiles, porcelain, and similar products.

Samples M1, M2, M3, and M4 exhibit moderate shrinkage, with plasticity indices of 24%, 27%, 31%, and 33%, all below 35%, making them suitable for extrusion. Therefore, with DON proportions of 5%, 10%, 15%, and 20% by mass, NTO clay can

be used for the manufacture of ceramic pieces.

3.2. Physicochemical Analysis of Ceramic Slips

3.2.1. Effect of Deflocculants on Ceramic Slips

This study investigates the influence of deflocculants on the stability of slips (ceramic pastes) prepared from NTO, DON, and their mixtures. For this purpose, we analyzed the pH and conductivity curves of the deflocculants (sodium hexametaphosphate and sodium metasilicate) as a function of the added clay amounts (0.15 g, 0.35 g, 0.55 g, 0.75 g, and 1 g).

- Influence of Sodium Hexametaphosphate on Slips Prepared from NTO and DON Clays: pH Evolution

Figure 5 shows the influence of sodium hexametaphosphate on NTO and DON clays.

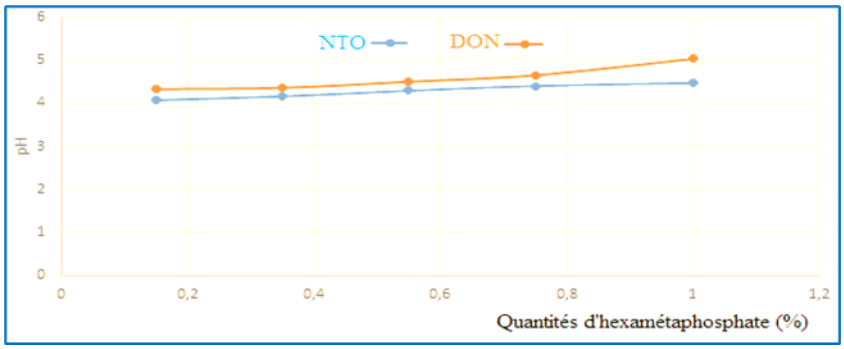

Figure 5: pH evolution as a function of the sodium hexametaphosphate percentage.

The addition of sodium hexametaphosphate, as shown in Figure 5, decreases the acidity of the suspensions. It is observed that the pH of the DON suspension is highly acidic, which does not favor good dispersion. This can be explained by the high presence of H_3O^+ ions in the medium: there is repulsion between the H_3O^+ ions and the positively charged edges of the clay particles. This prevents the adsorption of phosphate anions, causing the particles to form aggregates and promoting flocculation in the medium.

Phosphate anions (PO_4^{3-}), upon hydrolysis in the medium, are converted into ortho-phosphate anions. This reduces their deflocculating ability by preventing the precipitation of the multivalent Ca^{2+} cation present in the diffuse layer. This cation normally favors compression of the electrochemical double layer and also promotes attractive forces. As a result, instead of repelling each other for dispersion, the particles agglomerate to form a floc, thereby promoting flocculation of the suspension. The highly acidic medium compresses the electrochemical double layer further, enhancing flocculation.

Mineralogical analyses of NTO and DON had revealed the presence of trace oxides. This explains the inability of sodium hexametaphosphate to promote the dispersion of colloidal particles. Therefore, this deflocculant may cause issues such as cracking and deformation of ceramic products. These findings are consistent with the results reported by Ali Assifaoui (2002).

- **Evolution of Conductivity as a Function of Sodium Hexametaphosphate Percentage**

Figure 6 illustrates the change in conductivity as a function of the sodium hexametaphosphate percentage.

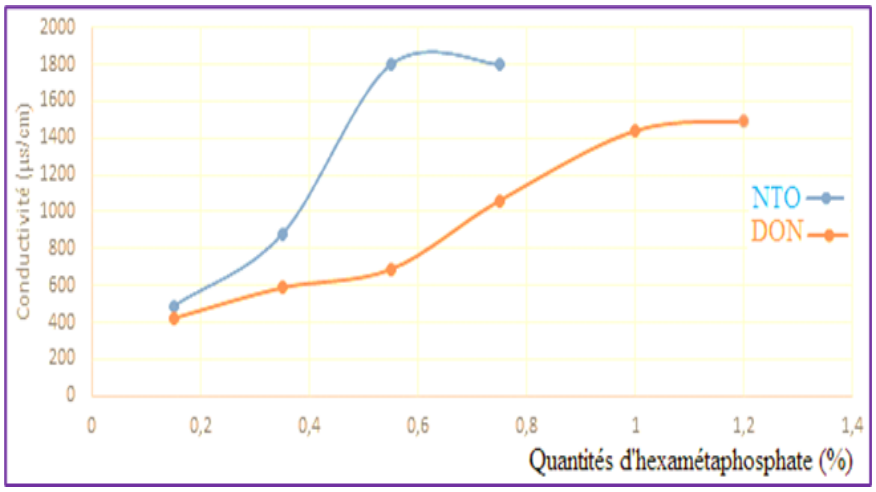

Figure 6: Evolution of conductivity as a function of sodium hexametaphosphate percentage

An increase in conductivity is observed in the NTO and DON curves (Figure 6). However, since sodium hexametaphosphate is rich in phosphate ions (soluble ions with low ionic strength), it does not promote a good suspension, especially in DON. This explains the relatively low conductivity compared to that reported by Ali Assifaoui (2002).

- Influence of Sodium Hexametaphosphate on Slips Prepared from M1, M2, M3, M4, and M5 Clays: pH Evolution

Figure 7 shows the influence of sodium hexametaphosphate on suspensions prepared from the mixtures.

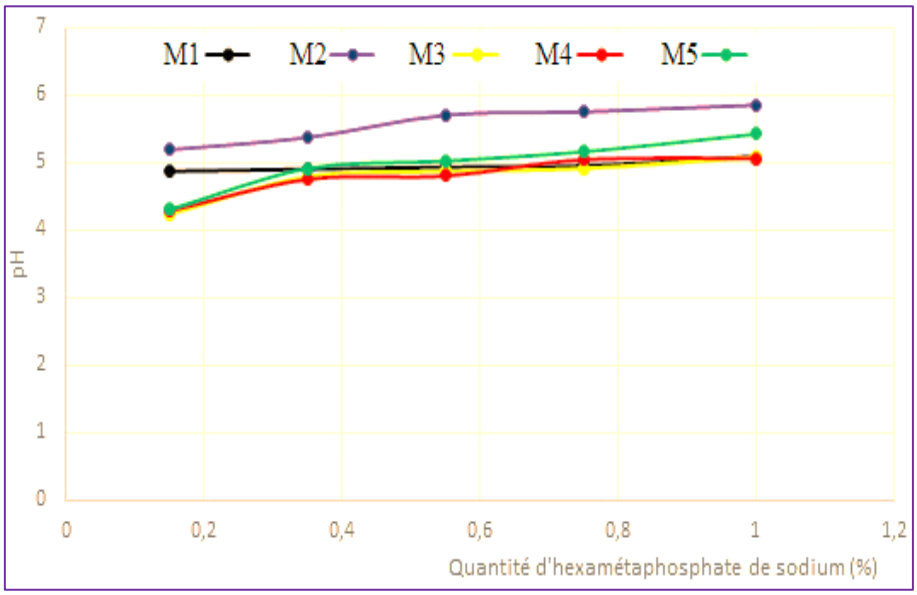

Figure 7: pH evolution as a function of sodium hexametaphosphate percentage

The addition of sodium hexametaphosphate, as shown in Figure 7, decreases the acidity of the suspensions. The pH of the suspensions ranges from 4.23 to 5.85.

- Evolution of Conductivity as a Function of Sodium Hexametaphosphate Percentage

Figure 8 shows the evolution of conductivity as a function of the sodium hexametaphosphate percentage.

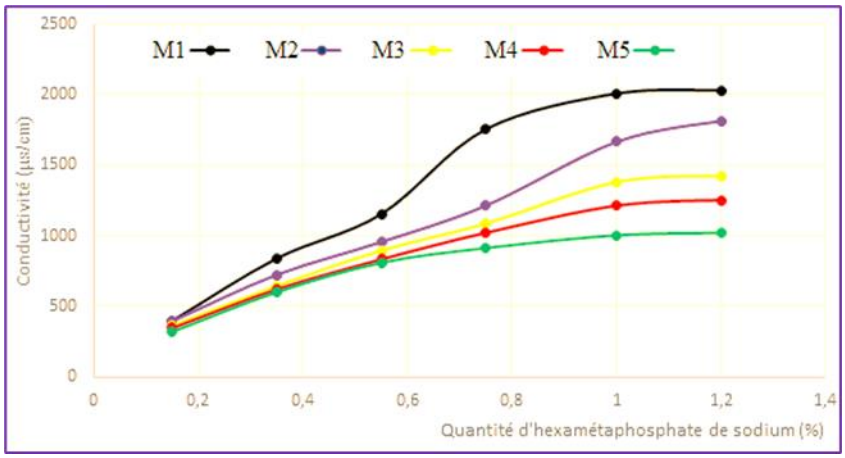

Figure 8: Evolution of conductivity as a function of sodium hexametaphosphate percentage

The addition of sodium hexametaphosphate also increases the conductivity of the mixtures' suspensions, as shown in Figure 8. The difference compared to sodium metasilicate is that sodium hexametaphosphate contains more soluble ions (phosphate ions) with low ionic strength, which does not promote good suspension conductivity. This explains the lower conductivity compared to that obtained with sodium metasilicate.

- **Influence of Sodium Metasilicate on Slips Prepared from M1, M2, M3, M4, and M5 Clays: pH Evolution**

Figure 9 illustrates the evolution of pH as a function of the sodium metasilicate percentage.

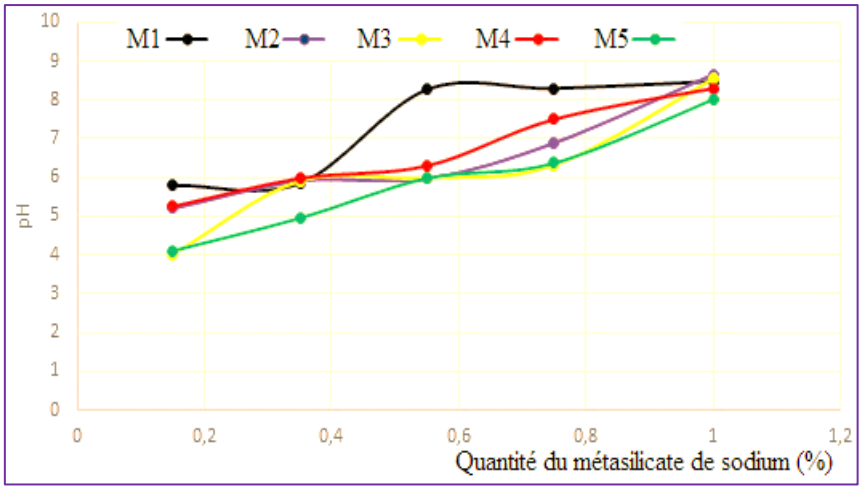

Figure 9: pH evolution as a function of sodium metasilicate percentage

The pH of the suspensions ranges from 4 to 8.70. Distilled water initially had a pH of 6.2 (slightly acidic). By adding silicate ions (SiO_4^{2-}), the suspensions become basic, which promotes dispersion. This is confirmed by peptization, which is the stable suspension of clay particles through the addition of peptizing ions (in this case, silicate ions).

- **Evolution of Conductivity as a Function of Sodium Metasilicate Percentage**

Figure 10 shows the evolution of conductivity as a function of the sodium metasilicate percentage.

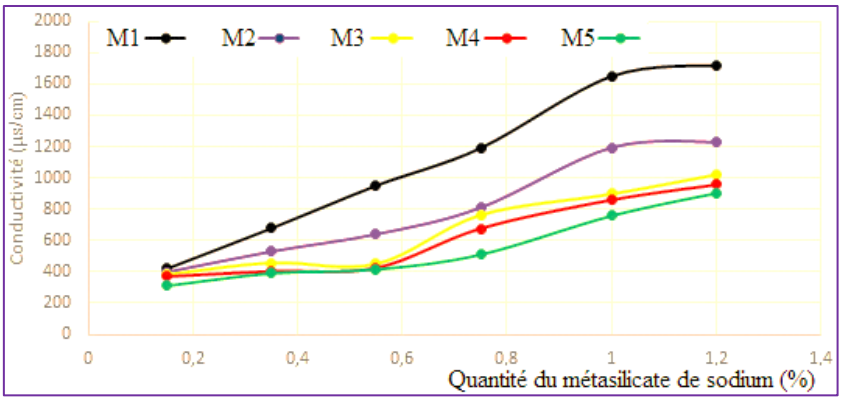

Figure 10: Evolution of conductivity as a function of sodium metasilicate percentage

The addition of sodium metasilicate, as shown in Figure 10, progressively increases the conductivity of the mixtures' suspensions. This result is expected since sodium metasilicate hydrolyzes into silicate anions. These ions increase the ionic strength of the suspension and promote very effective deflocculation.

3.3. Chemical Analysis

The chemical composition is presented in terms of major oxides in Table 2.

Table 2: Chemical composition (in % oxide by mass) of DON clay materials

Specimen	SiO_2	Al_2O_3	Fe_2O_3	MnO	MgO	CaO	Na_2O	K_2O	TiO_2	P_2O_5	PF	Total
NTO	71.28	16.19	1.63		0.12		0.02	0.36	1.43		9.04	100.07
DON	49.92	28.27	2.93	-	1.04	0.13	-	-	-	-	11.1	93.39

Table 2 presents the results of the chemical analysis of major elements (Si, Al, Fe, Mn, Mg, Ca, Na, K, Ti, and P) expressed as the percentage of the most stable oxide.

Structural Analysis

3.3.1. Thermal Behavior of the Mixtures

Here, we study the structural transformations as a function of firing temperatures (1100 and 1150°C) using X-ray diffraction. We observed two categories of materials: those (M1, M2, and M3) with plasticity indices below 50%, and those (M4 and M5) with plasticity indices above 50%. Accordingly, we formulated two mixtures (Table 3) to better understand their thermal behavior.

Table 3: Mixtures ND1 and ND2

Formulation No.	Mixture	Samples		Temperature (°C)
		NTO (%)	DON (%)	
1	ND1-1100	90	10	1100
	ND1-1150	90	10	1150
2	ND2-1100	50	50	1100
	ND2-1150	50	50	1150

These behaviors are illustrated by the X-ray diffraction patterns of the mixtures. Figure 11 presents these diffractograms.

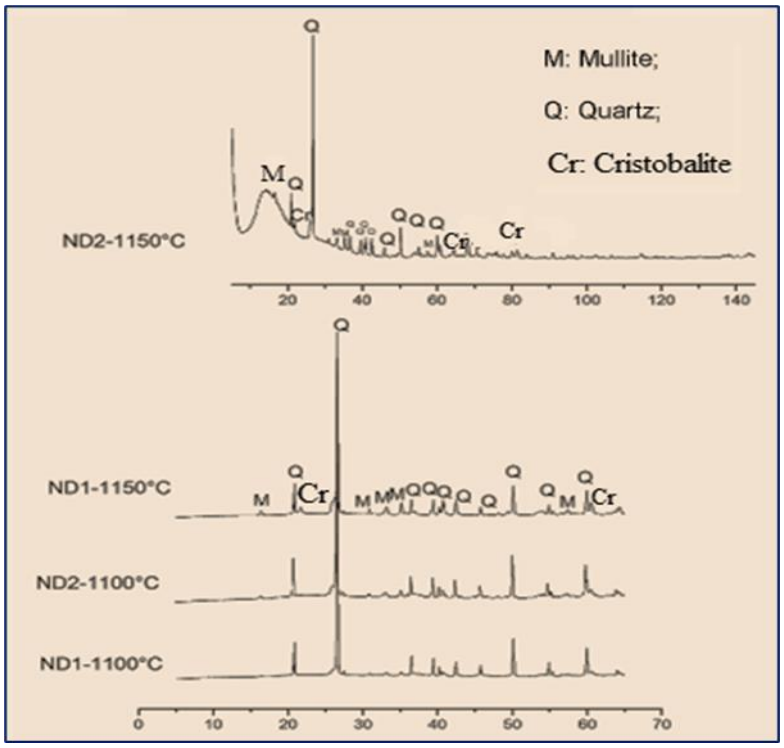

Figure 11: X-ray diffraction pattern of the mixture

Mullite is clearly present at high temperatures. The degree of crystallinity is remarkable, which enhances the mechanical properties of the ceramics (Farmer et al., 1995; Esharghawi et al., 2009).

3.4. Study of the Technological Properties of the Mixtures

3.4.1. Linear Shrinkage of ND1 and ND2 during Firing

Figure 12 shows the linear shrinkage of the mixtures during firing.

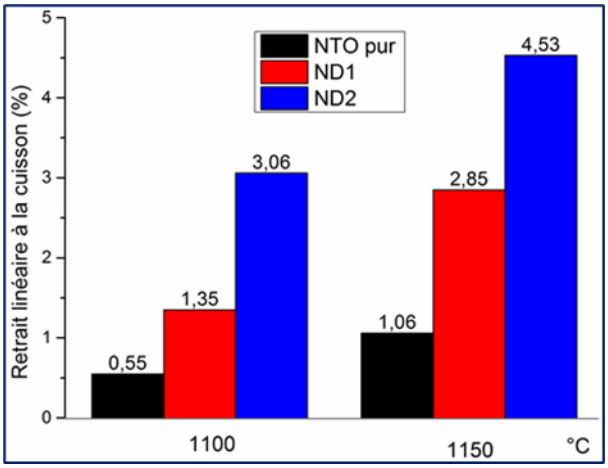

Figure 12: Linear shrinkage of ND1 and ND2 during firing as a function of temperature

We observed that after firing sample ND1 at 1150°C, the shrinkage increased by 1.50% compared to the value obtained (1.35%) after firing at 1100°C; for ND2, the increase was 1.47% after firing at 1150°C. In contrast, for the pure NTO sample, the shrinkage was very low (0.51%). The low shrinkage of Ntokou clay is likely due to the presence of quartz. Therefore, the addition of Dongou clay to Ntokou improved the properties of Ntokou.

3.4.2. Water Absorption Rate

Figure 13 shows how the water absorption rate evolves.

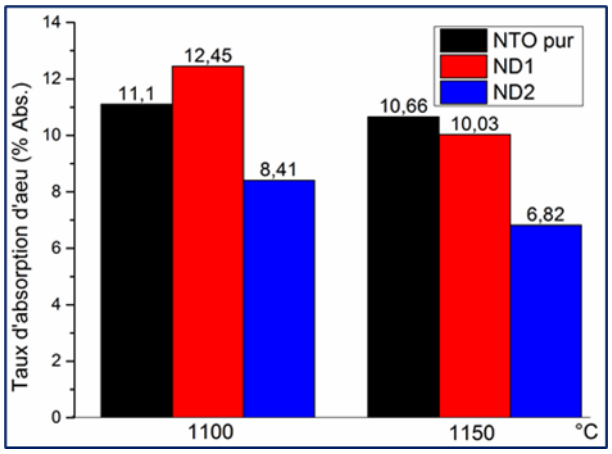

Figure 13: Water absorption rate of ND1 and ND2 as a function of temperature

From Figure 13, we observe a decrease of 2.42% for ND1 after firing at 1150°C, and a decrease of 1.59% for ND2 after firing at 1150°C. There is almost no reduction for pure NTO after firing at 1150°C (0.44%). This confirms the reduction in porosity and the consolidation of the grains, which is consistent with the SEM observations. We can conclude that the addition of Dongou clay was beneficial for Ntokou.

3.5.3. Three-Point Flexural Strength

Figure 14 shows the evolution of the three-point flexural strength.

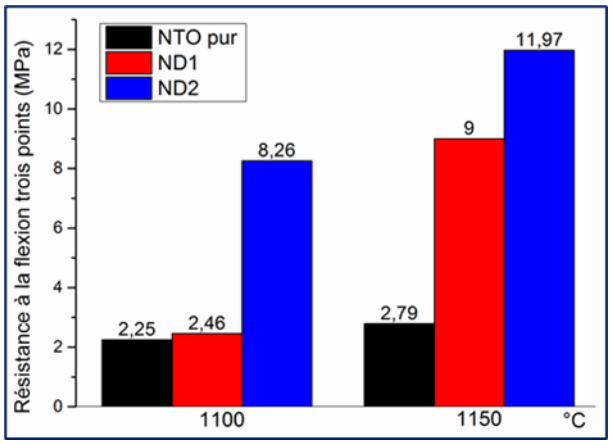

Figure 14: Three-point flexural strength of ND1 and ND2 as a function of temperature

We observe a significant increase in mechanical strength at 1150°C compared to that obtained at 1100°C for samples ND1 and ND2. This confirms the densification of the ND1 and ND2 ceramics. It can be concluded that the addition of Dongou clay improved the mechanical strength of Ntokou clay.

3.5. Microstructures Formed after Firing of ND1 and ND2 Samples at 1100 and 1150°C

Figure 15 shows SEM micrographs of the ND1 and ND2 samples, from which the size, morphology, and distribution of microstructures in these samples after firing at 1100 and 1150°C can be observed.

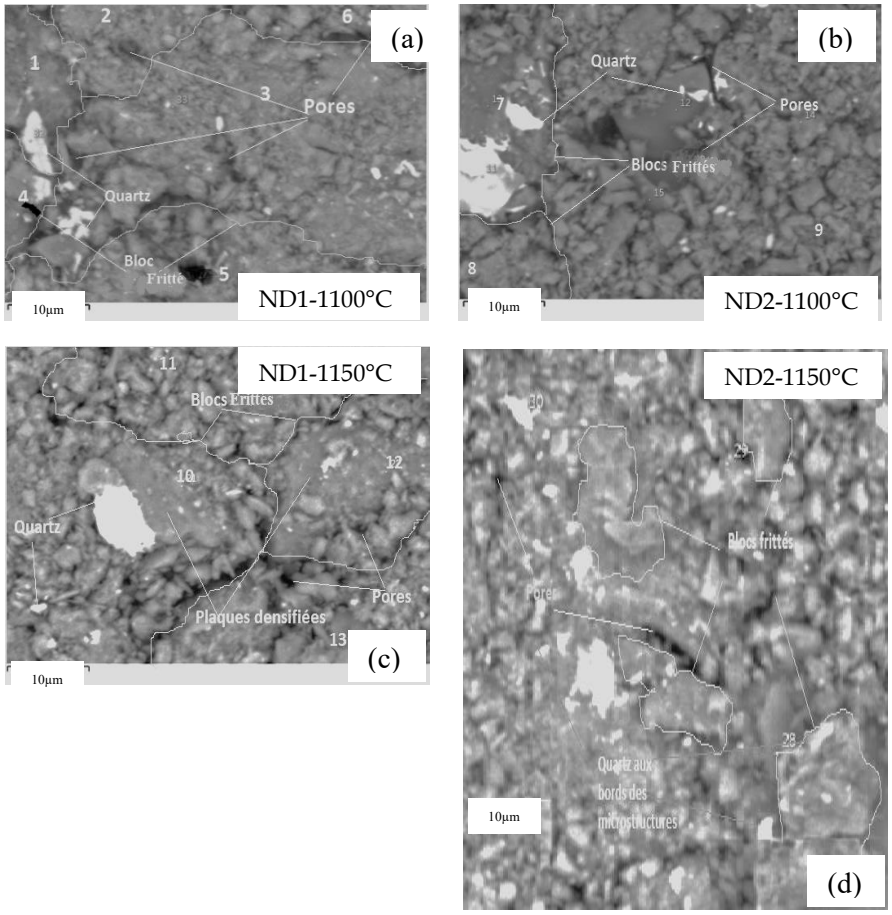

Figure 15 : Microstructures observées après cuisson des échantillons ND1 et ND2

The analysis of the SEM micrographs of ND1 and ND2 samples revealed the size, morphology, and distribution of microstructures in these samples after firing at 1100 and 1150°C. As observed in Figures 15 (a, b, and c), the grains are stacked, irregularly shaped, and adhered to each other along their common surfaces, with interconnected porosity and the absence of alkali and alkaline-earth oxides in these materials. This indicates viscous-flow sintering, due to impurities from the raw material.

It was also observed that between 1100 and 1150°C, the water absorption rate decreased by 2.42% for ND1 (from ND1-1100°C to ND1-1150°C) and by 1.59% for ND2 (from ND2-5 to ND2-6). Similarly, comparing water absorption rates for ND1-5 and ND2-5 at 1100°C and ND1-6 and ND2-6 at 1150°C, decreases of 4.04% and 3.21% were observed, respectively. In all cases, the water absorption decreased, indicating a reduction in open porosity and a progressive densification of the material.

A heterogeneous microstructure was observed in all micrographs (Figures 15 a, b, c, and d), with the coexistence of large and small grains. This suggests that some grains grew significantly at the expense of smaller grains (Figures 15 b, c, and d), a phenomenon described by Boch as discontinuous or abnormal grain growth. Such microstructures lead to unfavorable properties, as discontinuous grain growth hampers densification. The micrographs indicate that full densification was not achieved; although interconnected porosity is reduced, it remains partially open. Boch noted that porosity interconnection disappears when densification exceeds 90–92%. This explains the relatively low three-point flexural strength values of the fired ceramics (ND1-1100°C: 2.46 MPa; ND2-1100°C: 8.26 MPa; ND1-1150°C: 9 MPa; ND2-1150°C: 11.97 MPa).

Additionally, the poor densification may be due to the firing temperature, as other studies (e.g., Pialy, Diata) report complete densification at 1300°C. Therefore, firing at around 1200°C might achieve better densification. White spots were also observed on the grains and grain edges, similar to those in the SEM micrographs of Diata, Pialy, and Elimbi, corresponding to quartz. The presence of quartz in the material can hinder densification by forming a rigid skeleton that resists particle consolidation (Pialy et al., 2009).

It was noted that as open porosity decreased, larger grains formed, likely aided by iron and titanium forming a viscous liquid. Comparing ND1 and ND2 at 1100°C with those at 1150°C, the quartz content significantly decreased while the clay particles increased, explaining the observed shrinkage in ND2 samples (3.06% at 1100°C and 4.53% at 1150°C).

Overall, the addition of Dongou clay to Ntokou clay improved its properties. Pure NTO exhibited a shrinkage of 0.55%, water absorption of 11.10%, and flexural strength of 2.25 MPa at 1100°C (Moutou et al., 2020). In comparison, ND1 had a shrinkage of 1.35%, water absorption of 12.45%, and flexural strength of 2.46 MPa, while ND2 had a shrinkage of 3.06%, water absorption of 8.41%, and flexural strength of 8.26 MPa at 1100°C. Similar improvements were observed at 1150°C.

4. CONCLUSION

This study investigated the thermomechanical behavior of a mixture of two clay soils. Improving the mechanical properties of NTO clay required the addition of DON clay in proportions of 5%, 10%, 15%, 20%, and 25%, resulting in mixtures M1, M2, M3, M4, and M5. Atterberg limits confirmed the clayey nature of M1–M5 and allowed their classification: M1 and M2 as medium-plastic clays with unfavorable molding properties, and M3, M4, and M5 as highly plastic clays with optimal molding properties.

In slip preparation, sodium metasilicate promoted deflocculation, whereas sodium hexametaphosphate favored flocculation. Mixtures M4 and M5 exhibited low permeability and porosity, providing significant flexural strength. Mullite was identified by X-ray diffraction. Technological properties improved in ND1 and ND2 at 1150°C compared to pure NTO.

Declaration by Authors

Acknowledgement: None
Source of Funding: None
Conflict of Interest: No conflicts of interest declared.

5. REFERENCES

1. Afnor, N. (1996). NFP 94-056, Sols : reconnaissance et essais-Analyse granulométrique-Méthode par tamisage à sec après lavage. Association Française de Normalisation France.
2. Afnor, N. F. (1993). Sols : reconnaissance et essai ; détermination des limites d'atterberg. Limite de liquidité à la coupelle Limite de plasticité au rouleau.
3. Assifaoui, A. (2002). Etude de la stabilité de barbotines à base d'argiles locales: application aux formulations céramiques industrielles (Doctoral dissertation, éditeur inconnu).
4. Bain, J.A. and D.E. Highly, 1978. Regional appraisal of clay resources: Challenge to the clay mineralogist. In: Mortland, M.M. and V.C. Faxmer (Eds.), Proc. Int. Clay Conference. Elsevier, Amsterdam, pp: 437-446.
5. Capitâneo, J.L., F.T. Da Silva, C.M.F. Vieira and S.N. Monteiro, 2005. Reformulation of a kaolinitic body for extruded floor tiles with phonolite addition. Sil. Ind., 70(11-12): 161-165.
6. Casagrande, A., 1948. Classication and identification of soils. T. Am. Soc. Civil Eng., 113: 901-930.
7. Diatta, M. T., Lecomte-nana, G. L., Kobor, D., Sock, O., Blanchart, P., et Azilinon, D. (2015). developpement of ceramics silicates-based clays of Senegal: physicochemical caharacteristics and consolidation. *Proc. Plumee*, *1*, 41-44.
8. Duplan, Y., et Forquin, P. (2021). Investigation of the multiple-fragmentation

process and post-fragmentation behaviour of dense and nacre-like alumina ceramics by means of tandem impact experiments and tomographic analysis. International Journal of Impact Engineering, 155, 103891.

9. El Boukili, G., Lechheb, M., Ouakarrouch, M., Dekayir, A., Kifani-Sahban, F. et Khaldoun, A. (2021). Caractérisation minéralogique, physico-chimique et technologique de l'argile de Bensmim (Maroc) : Aptitude à l'application en bâtiment. Construction et matériaux de construction, 280, 122300.
10. Esharghawi A, Penot C, Nardou F. Contribution to Porous Mullite Synthesis from Clays by Adding Al and Mg Powders. Journal of the European Ceramic Society. 2009 ; Vol. 29, No. 1, pp 31-38.
11. Farmer, V. C. (1974). The Infrared Spectra of Minerals. Mineralogical society monograph, 4, 331-363.
12. Lecomte, N. K., et Laure, G. (2004). Transformations thermiques, organisation structurale et frittage des composés kaolinite-muscovite (Doctoral dissertation, Limoges).
13. NF EN 843-1 – Céramiques techniques avancées – Propriétés mécaniques des céramiques monolithiques à température ambiante – Partie 1 : détermination de la résistance à la flexion.
14. Pialy, P., Tessier-Doyen, N., Njopwouo, D., et Bonnet, J. P. (2009). Effects of densification and mullitization on the evolution of the elastic properties of a clay-based material during firing. Journal of the European Ceramic Society, 29(9), 1579-1586.
15. Samara, M. (2007). Valorisation des sédiments fluviaux pollués après inertage dans la brique cuite (Thèse de doctorat, Ecole Centrale de Lille).

How to cite this article: Banzouzi Samba Vivien Igor, Nzaba-Madila Erman-Eloge, Vezolo Stanislas Prudence, Bibila Mayaya Bisseyou Yvon, Moutou Jospeh-Marie Saint Bastia, Elimbi Antoine. Study of the thermomechanical behavior of a mixture of two aluminosilicate powders. *International Journal of Research and Review*. 2026; 13(1): 373-386. DOI: *https://doi.org/10.52403/ijrr.20260135*

******